



HAL
open science

Genetic Determinants of Individual Variation in the Superior Temporal Sulcus of Chimpanzees (*Pan troglodytes*)

William Hopkins, Oliver Coulon, Adrien Meguerditchian, Nicky Staes, Chet Sherwood, Steven Schapiro, Jean-Francois Mangin, Brenda Bradley

► **To cite this version:**

William Hopkins, Oliver Coulon, Adrien Meguerditchian, Nicky Staes, Chet Sherwood, et al.. Genetic Determinants of Individual Variation in the Superior Temporal Sulcus of Chimpanzees (*Pan troglodytes*). *Cerebral Cortex*, 2022, <10.1093/cercor/bhac183>. <hal-03871725>

HAL Id: hal-03871725

<https://hal.science/hal-03871725v1>

Submitted on 25 Nov 2022

HAL is a multi-disciplinary open access archive for the deposit and dissemination of scientific research documents, whether they are published or not. The documents may come from teaching and research institutions in France or abroad, or from public or private research centers.

L'archive ouverte pluridisciplinaire **HAL**, est destinée au dépôt et à la diffusion de documents scientifiques de niveau recherche, publiés ou non, émanant des établissements d'enseignement et de recherche français ou étrangers, des laboratoires publics ou privés.



HAL Authorization

Genetic Determinants of Individual Variation in the Superior Temporal Sulcus of Chimpanzees (*Pan troglodytes*)

William D. Hopkins*^{1,2,3} Oliver Coulon^{3,4}, Adrien Meguerditchian^{3,5}, Nicky Staes⁶, Chet C. Sherwood⁶, Steven J. Schapiro^{1,7}, Jean-Francois Mangin⁸, & Brenda Bradley⁶

¹ Department of Comparative Medicine, The University of Texas MD Anderson Cancer Center, Bastrop, Texas 78602

² IMÉRA – Institut d’Etudes Avancées, Aix-Marseille Université, 13004 Marseille, France

³ Institute of Language, Communication and the Brain, Aix-Marseille Université, CNRS, 13604 Aix-en-Provence, France

⁴ Aix-Marseille Univ, CNRS, Institut de Neurosciences de La Timone, UMR7289 Marseille, France

⁵ Laboratoire de Psychologie Cognitive, UMR 7290, LPC, Aix-Marseille Univ, CNRS, Marseille, France

⁶ Department of Anthropology and Center for the Advanced Study of Human Paleobiology, The George Washington University, Washington, DC 20052

⁷ Department of Experimental Medicine, University of Copenhagen, Copenhagen, Denmark

⁸ Paris-Saclay University, CEA, CNRS, Neurospin, Saclay, France

Abstract

The superior temporal sulcus (STS) is a conserved fold that divides the middle and superior temporal gyri. In humans, there is considerable variation in the shape, folding pattern, lateralization and depth of the STS that have been reported to be associated with social cognition and linguistic functions. We examined the role that genetic factors play on individual variation in STS morphology in chimpanzees. The surface area and depth of the STS were quantified in sample of 292 captive chimpanzees comprised of two genetically isolated population of individuals. The chimpanzees had been previously genotyped for AVPR1A and KIAA0319, two genes that play a role in social cognition and communication in humans. Single nucleotide polymorphisms in the KIAA0319 and AVPR1A genes were associated with average depth as well as asymmetries in the STS. By contrast, we found no significant effects of these KIA0319 and AVPR1A polymorphism on surface area and depth measures for the central sulcus. The overall findings indicate that genetic factors account for a small to moderate amount of variation in STS morphology in chimpanzees. These findings are discussed in the context of the role of the STS in social cognition and language in humans and their potential evolutionary origins.

The superior temporal sulcus (STS) is a highly conserved fold of the cerebral cortex in primate brains that divides the superior and middle gyri of the temporal lobe (Connolly 1936; Connolly 1950) (see Figure 1). In cercopithecoid and platyrrhine monkeys, the STS is largely a smooth fold that begins at the temporal pole and extends posteriorly beyond the most posterior point of the Sylvian fissure and terminates in the parietal lobe. In great apes and humans, there is considerably more variation in the shape and trajectory of the STS, particularly in the posterior region where, posterior and dorsal to the terminal point of the Sylvian fissure, the sulcus can bifurcate into descending and ascending limbs that may or may not be connected to the primary fold (see Figure 2). Further, in humans, and to a lesser extent in chimpanzees, the STS may be split into multiple sections or pieces due to the presence of “pli-de-passages” or buried gyri (Bodin et al. 2021), which has been reported to be more frequently found in the left compared to the right hemisphere in humans (Le Guen et al. 2018). Recently, it has been suggested that asymmetries in the central region of the STS, referred to as the STAP (**S**uperior **T**emporal **A**symmetric **P**it), are a human-specific anatomical landmark that has been hypothesized to be linked to the evolution of language. Specifically, LeRoy et al. (2015) quantified the depth of the STS in regions anterior and posterior to Heschl’s gyrus in MRI scans of humans and chimpanzees and reported robust, rightward asymmetries in the STAP region in human subjects, whereas chimpanzees showed a relatively small, and only marginally significant rightward bias. These findings are particularly interesting because previous studies in chimpanzees have reported population-level asymmetries in the perisylvian region, including the posterior STS and planum temporale; results that are quite similar to those in humans

(Hopkins and Nir 2010; Kong et al. 2018; Spocter et al. 2020). Thus, given the role of the posterior STS and superior temporal gyrus (STG) in a variety of linguistic, socio-communicative and cognitive functions (i.e., such as the processing of faces, auditory stimuli and biological motion) (Redcay 2008; Deen et al. 2015; Specht and Wigglesworth 2018) and the purported human uniqueness of asymmetries in the STAP, further studies on the morphology of the STS in other primate species are warranted as a means of characterizing the evolution of this cortical fold, as well as factors that influence individual variation in its expression.

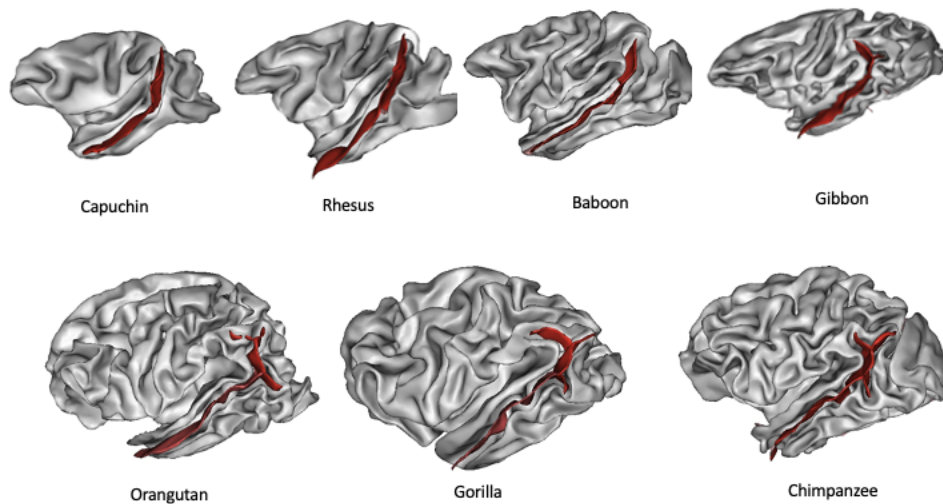


Figure 1: 3D lateral views of the superior temporal sulcus (STS) in different primate species.

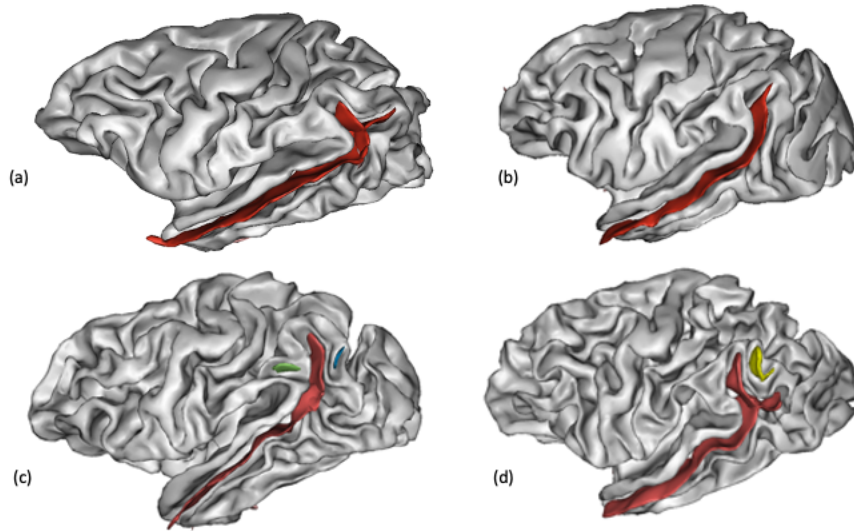


Figure 2: Four different example of variation in the morphology of the STS. (a) typical pattern with a bifurcated anterior and posterior limb (b) less common variants with no bifurcation at the posterior terminal position (c) STS variant with a disconnected anterior (green) and posterior (yellow) limb (d) STS variant with an intermediate fold (yellow).

To this end, we examined the contribution of genetic and non-genetic (environmental) factors to individual variation in the surface area, mean depth and the depth profile along the length of the STS in chimpanzees. In the initial set of analyses, we divided the entire STS into anterior and posterior regions and quantified the overall surface area and mean depth. We next quantified the depth profile of the anterior STS, which included the STAP region, in the left and right hemispheres in the chimpanzee sample. From these data, in one analysis, we tested for population-level asymmetries as a means of evaluating their uniqueness as hypothesized by LeRoy et al. (2015). In a second set of analyses, following methods used in previous studies with human and nonhuman primates (Rogers et al. 2007; Fears et al. 2009; Rogers et al. 2010; McKay et al. 2013; Hopkins, Coulon, Meguerditchian, Autrey, Davidek, Mahovetz, Pope, et al. 2017; Hopkins et al. 2018; Hopkins et al. 2019), we used quantitative genetic analyses

based on the available pedigree information for the chimpanzees to estimate heritability in the STS regions, as well as the contribution of non-genetic factors including their sex, age, rearing history and the magnet strength of the scanner used to obtain the images. One unique aspect of the chimpanzee sample was that it was comprised of two cohorts of apes that were founded by separate wild-born animals and their descendants were raised at two different research facilities with no transfer of individuals between them. Thus, the two cohorts were genetically isolated from each other and this allowed us to evaluate the repeatability of the heritability results.

We also examined whether polymorphisms in two different genes were implicated in individual variation in STS morphology. In one set of analyses, we tested whether single nucleotide polymorphisms (SNPs) in the *KIAA0319* gene potentially explain individual variation in the STS and, specifically in the STAP region. *KIAA0319* is a gene strongly implicated in language functions and polymorphisms in this gene have been repeatedly implicated in developmental dyslexia (DD) in humans, a reading disorder that is primarily manifest in difficulties learning associations between sounds with letters and/or words (Cope et al. 2005; Dennis et al. 2009; Scerrl et al. 2011). Meta-analyses have shown that individuals with DD show atypical patterns of gray matter volume, cortical thickness and white matter connectivity in brain regions implicated in language (Eckert et al. 2016; Eicher et al. 2016). Studies in humans have also shown that SNPs in the *KIAA0319* gene are associated with the prevalence of DD and are linked to differences in grey and white matter cortical organization, particularly within the posterior superior-temporal lobe and parietal junction within the left hemisphere (Robichon et al. 2000; Darki et al. 2012; Pinel et al. 2012). Similarly, in

chimpanzees, a recent study identified two SNPs in the *KIAA0319* gene that were associated with individual variation in gray matter covariation in the posterior superior temporal gyrus (Hopkins et al. in press). For this reason, we hypothesized that these same polymorphisms might also be associated with variation in the surface area and depth of the chimpanzee STS.

We also tested for associations between polymorphisms in the gene coding for arginine vasopressin receptor 1A, *AVPR1A*, and variation in STS morphology. *AVPR1A* has been shown to play a role in social behavior and cognition in mammals (Goodson and Bass 2001; Donaldson and Young 2008; French et al. 2016; Hopkins and Latzman 2021) and has been hypothesized to be a candidate gene for psychological disorders in which deficits in social behavior are prominent, such as autism spectrum disorder (ASD) (Hammock and Young 2006; Yirmiya et al. 2006; Carter 2007; Donaldson and Young 2008; Melke 2008; Francis et al. 2016; Parker et al. 2018). Consistent with this view, neuroimaging studies have shown that gray matter volume and white matter connectivity in the STS differ between individuals with and without a diagnosis of ASD (Zilbovicius et al. 2006) and other neuropsychiatric disorders (Plaze et al. 2011). Previous studies have shown that chimpanzees possess an indel deletion in the *AVPR1A* microsatellite, resulting in a bimodal distribution of subjects with (DupB+/-) or without (DupB-/-) the RS3 duplication (Hammock 2005; Donaldson et al. 2008). Behaviorally, DupB+/- (which can include a small cohort of DupB+/+ individuals) and DupB-/- chimpanzees have been found to differ significantly in dimensions of personality and social behavior (Hopkins et al. 2012; Anestis et al. 2014; Latzman et al. 2014; Staes et al. 2014; Wilson et al. 2017). For example, Mahovetz et al. (2016)

recorded the social behavior of chimpanzees when presented with a mirror and found that DupB+/- males showed higher rates of scratching (reflecting anxiety) and agonistic behaviors compared to DupB-/- males and both DupB+/- and DupB-/- females.

Polymorphisms in AVPR1A are also associated with a composite score reflecting ASD phenotypes (Weiss et al. 2021) as well as social cognition measures linked to ASD, notably receptive joint attention (RJA) (Hopkins, Keebaugh, et al. 2014). Previous studies have also found that both humans and chimpanzees with poor joint attention skills differ in gray matter volume of the posterior, but not anterior, portion of the superior temporal gyrus (Hopkins, Misiura, et al. 2014; Mundy 2018). Finally, Mulholland et al. (2020) using source-based morphometry, found that DupB-/- chimpanzees had significantly higher covariation in gray matter within the superior temporal gyrus compared to DupB+/- apes. In light of the significant differences found between DupB+/- and DupB-/- apes in behavior and gray matter covariation within the superior temporal gyrus, we hypothesized that chimpanzees with these two genotypes would also differ on measures of STS surface area and depth.

Finally, we tested whether the influence of polymorphisms in the KIAA0319 and AVPR1A were specific to the STS. To test this hypothesis, we examined the influence of polymorphisms in KIAA0319 and AVPR1A on depth and surface area measures of the central sulcus (CS). The surface area and depth of the CS in chimpanzees has been previously reported to be significantly heritable and associated with manual and oro-facial motor skills in this same chimpanzee sample (Hopkins, Coulon, Meguerditchian, Autrey, Davidek, Mahovetz, S., et al. 2017). If the influence of polymorphisms in the KIAA0319 and AVPR1A genes were specific to the STS, then we

hypothesized that no significant effects would be found for the surface area and depth of the CS.

Methods

Subjects

For the quantitative genetic analyses on STS heritability, magnetic resonance images (MRI) were obtained from 292 captive chimpanzees housed at either the Yerkes National Primate Research Center (YNPRC, $n = 133$) or the National Center for Chimpanzee Care (NCCC, $n = 157$) of The University of Texas MD Anderson Cancer Center. There were 170 females and 122 males ranging from 6 to 54 years of age (Mean = 27.99 years, $SD = 11.11$). Within this sample, there were 136 mother-reared, 92 nursery-reared and 64 wild-born individuals. A breakdown in the composition of relatedness of the two chimpanzee samples has been previously reported in Hopkins, Reamer, et al. (2015). With the exception of two individuals, nursery-reared (NR) chimpanzees were separated from their mothers within the first 30 days of life, due to unresponsive care, sickness, or injury, and leaving them in their circumstance at the time would have increased the risk of death (Bard et al. 1992; Bard 1994). The NR chimpanzees were placed in incubators, fed standard human infant formula, and cared for by humans until they could sufficiently care for themselves, at which time they were placed with other infants of the same age until they were 3 years of age (Bard *et al.* 1992; Bard 1994). At 3 years of age, NR chimpanzees were integrated into larger social groups of adult and sub-adult chimpanzees. Mother-reared (MR) chimpanzees were not separated from their mother for at least the first 2.5 years of life and were raised in nuclear family groups ranging from 4 to 20 individuals. The two exceptions of NR

individuals were Lana and Panzee, chimpanzees that were born at the YNPRC but raised in a rich social-linguistic environment by humans at the Language Research Center (LRC) as part of an initiative to investigate the linguistic skills of chimpanzees (Rumbaugh 1977; Brakke and Savage-Rumbaugh 1995, 1996). Wild-born (WB) chimpanzees were individuals who had been captured in the wild and subsequently brought to research facilities within the United States prior to 1974, when the importation of chimpanzees was banned. All scanning procedures performed with the chimpanzees were approved by the local Institutional Animal Care and Use Committees and followed all recommendations by the Institute of Medicine for the ethical treatment of chimpanzees in research.

KIAA0319 and AVPR1A Genotypes

All genotyping was performed on DNA extracted from banked blood samples obtained from the chimpanzees during their annual physical examination within each facility prior to 2015. DNA samples were not available on the entire sample of 292 chimpanzees; thus, all analyses examining the influence of genotype on the STS involved fewer individuals. The details for DNA extraction, primer sequences and analyses have been provided in detail in previous publications (Hopkins *et al.* 2012; Hopkins *et al.* 2021). For *KIAA0319*, one SNP, RS_P1, had allele frequencies of 99 (AA), 104 (AT) and 46 (TT). For the second SNP, RS_63, the allele frequencies within our population were 78 (AA), 116 (AC) and 54 (CC). For *AVPR1A*, there were 85 DupB^{+/-} and 153 DupB^{-/-} within the sample.

MRI Image Collection

Both *in vivo* (n = 228) and *ex vivo* (n = 64) post-mortem MRI scan data were used in this study. *In vivo* scans were obtained at the time the chimpanzees were being surveyed for their annual physical examinations beginning in 1998 and continuing until 2014. Subjects were first immobilized by ketamine (10 mg/kg) or telazol (3-5mg/kg) and subsequently anaesthetized with propofol (40–60 mg/(kg/h)) following standard procedures at the YNPRC and NCCC facilities. YNPRC subjects were then transported to the MRI facility, while NCCC subjects were wheeled to a mobile imaging unit. The subjects remained anaesthetized for the duration of the scans, as well as the time needed to transport them between their home cage and the imaging facility (between 5 and 10 minutes) or mobile imaging unit (total time ~ 5 minutes). Subjects were placed in the scanner chamber in a supine position with their head fitted inside the human-head coil. Scan duration ranged between 40 and 60 minutes as a function of brain size.

Seventy-seven chimpanzees were scanned using a 3.0 Tesla scanner (Siemens Trio, Siemens Medical Solutions USA, Inc., Malvern, Pennsylvania, USA) at YNPRC. T1-weighted images were collected using a three-dimensional gradient echo sequence (pulse repetition= 2300 ms, echo time= 4.4 ms, number of signals averaged= 3, matrix size = 320 X 320). Additionally, 139 NCCC and 13 YNPRC chimpanzees were scanned using a 1.5 Tesla Phillips or GE machine. T1-weighted images were collected in the transverse plane using a gradient echo protocol (pulse repetition= 19.0 ms, echo time= 8.5 ms, number of signals averaged= 8, and a 256 x 256 matrix). After completing MRI procedures, the subjects were temporarily housed in a single enclosure for 6–12 h to allow the effects of the anesthesia to wear off, after which they were returned to their social group. Post-mortem T2-scans were obtained from 64 chimpanzees that had died

from natural causes. For the post-mortem scanning, either 4.7 or 7T magnets were used and T2-weighted images were collected in the transverse plane using a gradient echo protocol (pulse repetition = 22.0 s, echo time = 78.0 ms, number of signals averaged = 8-12, and a 256×192 matrix reconstructed to 256×256).

Sulci Extraction and Measurement

The sequence of post-image processing steps performed on the images are shown in Figures 3a to 3h and have been described in detail elsewhere (Hopkins et al. 2010; Bogart et al. 2014; Hopkins, Coulon, Meguerditchian, Autrey, Davidek, Mahovetz, S., *et al.* 2017). The processing used to extract the sulci from the raw T1-weighted image derives from a pipeline initially dedicated to the human brain and freely distributed as a BrainVISA toolbox (<http://brainvisa.info>) (Mangin et al. 2004). To account for the differences in chimpanzee anatomy compared to humans, a number of adjustments were performed before the scans were processed using the pipeline procedure within BrainVISA (BV). Specifically, chimpanzee MRI volumes were skull-stripped, cropped, denoised (Coupe et al. 2008), and reformatted at 0.625 mm isotropic resolution using ANALYZE 11.0 software and subsequently imported into BV. The pipeline process of extracting the sulci from the cortex involved a number of steps (Mangin *et al.* 2004) (see Figure 3a to 3h). To align the template brain, the anterior and posterior commissures were manually specified on the MRI at the point where they intersect with the mid-sagittal slice. The first step was to correct for spatial inhomogeneities in the signal intensity, providing a spatially smooth bias field with a stable distribution of tissue intensities (Figure 3b). Next, the analysis of the signal histogram and mathematical morphology were performed using an automatic analysis

of the voxel intensities for the entire brain to obtain a binary mask of the brain (Figure 3c). Adjustments were sometimes needed in the histogram process to determine gray and white matter means for chimpanzee brain scans. The mask was then split into the left and right hemispheres and the cerebellum (Figure 3d). A negative cast of the white matter was computed from the split-brain mask. The outside boundary of this cast results from a 5 mm morphological closing of the masked hemisphere, filling up the folds. The gray/white interface is the inside boundary and is computed using deformations that assure the spherical topology of the cast (Figure 3e). Finally the cast was skeletonised to detect cortical folding, while topological constraints guaranteed the resulting surfaces would have no holes (Mangin 2000; Mangin *et al.* 2004) (Figure 3f & 3g). The STS and the CS in each hemisphere was selected manually (Figure 3h) by the user, using a 3D visualization interface (Bailey *et al.* 1950; Hopkins, Meguerditchian, *et al.* 2014).

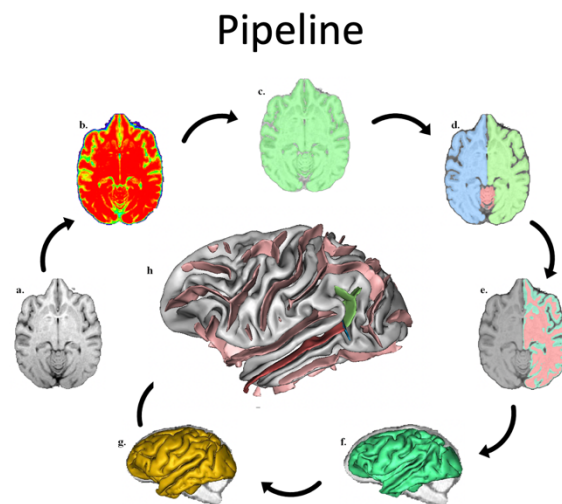


Figure 3: Pipeline process in BrainVisa for sulci extraction.

To divide the STS into its anterior and posterior sections, we used a sulcus that was present in the majority of brains (labelled as A3 in Connolly 1936) and could be used to divide the STS into anterior and posterior regions (see Figure 4). In more than 75% of the hemispheres, the BV pipeline produced a natural break in the STS at the A3 sulcus. In the absence of a natural break, we used the scissors tool in BV to manually bisect the fold along the medial-lateral axis of A3. Using this landmark, the STS was divided into the anterior (STS_Ant) and posterior (STS_Post) regions. For the STS_Post, we included all the folds that were dorsal to the STS_ventral, including those that were disconnected from the main STS fold. The STS_Post excluded any sulci that were part of the lunate, posterior central and intraparietal sulci. The STS_Ant and STS_Post were manually labelled for the left and right hemisphere and we calculated the surface area and mean depth for each region.

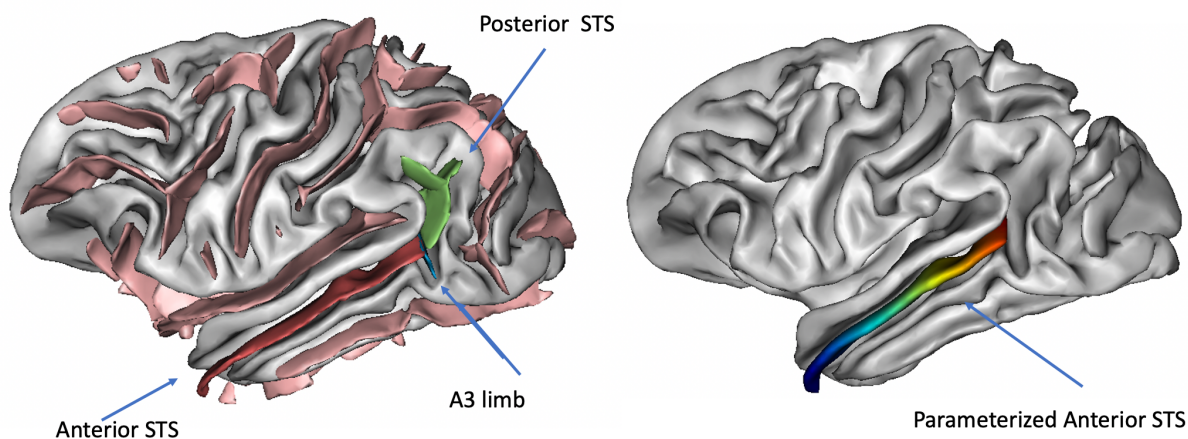


Figure 4: Left panel: 3D rendering of chimpanzee brains with the STS extracted and the landmarks identified to distinguish between the anterior and posterior sections. Right panel: 3D rendering of chimpanzee brain showing the STS_Ant section that the parameterization analyses were performed for each subject.

Parameterization of the STS_Ant

The selected STS_Ant was meshed using a triangular mesh, and the resulting surface was parameterized in order to create a longitudinal coordinate system (Coulon et al. 2015) (Figure 5a to 5d). The parameterization process was constrained by the anterior and posterior sulcus extremities, automatically detected using the extrema of the first non-zero eigenfunction of the mesh Laplacian (e_1 and e_2 , Fig. 5b). From these points, a smooth and quasi-isometric (i.e. with minimal metric distortions) coordinate field is extrapolated, that localizes all mesh surface points according to their relative position along the sulcus between the two extremities (Fig. 5c). The coordinate field extends along the length of the STS_Ant from the anterior ($y = 1$) to the posterior ($y = 100$) ends of the sulcus. Depth was measured at 100 sulcal length positions in an anterior-to-posterior progression along the parameterized sulcal mesh surface. Position 1 was located at the most anterior point of STS_Ant, while position 100 was located at the most posterior point of the STS_Ant where the A3 sulcus was located (see Fig 5c). At each position, y , along the length, the depth is computed by measuring a geodesic distance (in millimeters) from the brain envelope to the fundus of the sulcus (Fig. 5d). To simplify the analyses, within the left and right hemispheres, we averaged every 5 depth measures from point 0 to 100 to create 20 STS_Ant regions along the anterior-posterior plane.

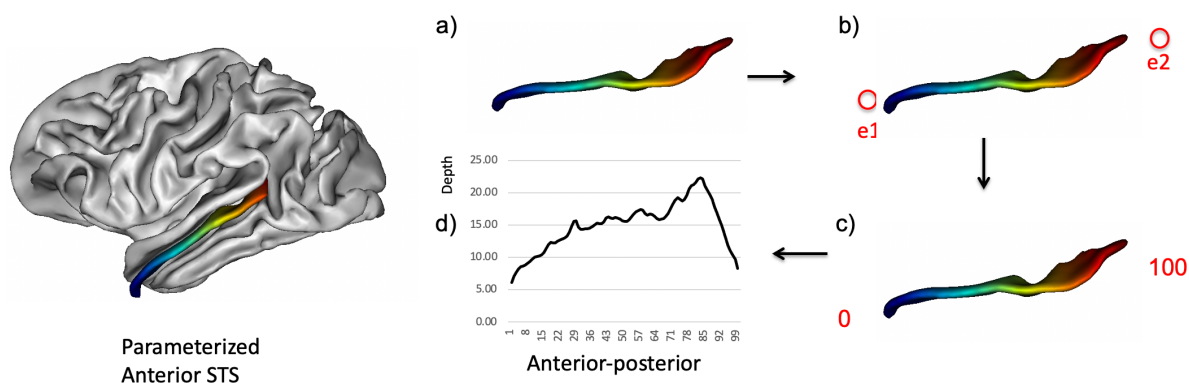


Figure 5: Parameterization steps of the STS_Ant of the chimpanzee brain (see text for description).

Heritability Analyses

Consistent with previous studies, we used the software package SOLAR to estimate heritability in the STS (Almasy and Blangero 1998) (<http://solar-eclipse-genetics.org>). SOLAR uses a variance component approach to estimate the polygenic component of variance when considering the entire pedigree (see Rogers *et al.* 2007; Fears *et al.* 2009; Fears *et al.* 2011; Hopkins, Keebaugh, *et al.* 2014). Total additive genetic variance (h^2) is the amount of total phenotypic variance that is attributable to all genetic sources. Total phenotypic variance attributable to genetic and non-genetic variables is constrained to a value of 1; therefore, all non-genetic contributions to the phenotype are equal to $1 - h^2$. We used SOLAR to determine heritability in the average surface area and average depth of the overall STS_Ant and STS_Post regions by adding the left and right hemisphere values and dividing by two. We also computed an asymmetry quotient (AQ) for the surface area and mean depth measures for both the STS_Ant and STS_Post region following the formulas $[AQ = (R - L) / ((R + L) * .5)]$

where R and L represent the right and left hemisphere values. Positive AQ values indicated rightward and negative values indicated leftward biases. We also used SOLAR to estimate heritability in the STS_Ant depth values based on the parameterization data by calculating the average for the right and left hemisphere and AQ values for each of the 20 regions. For all heritability analyses, scanner strength (1.5T, 3T, and 7T), sex, age, and rearing history served as covariates in the analyses. Heritability estimates and genetic correlations at $p \leq .05$ were considered significant.

Results

Quantitative Genetic Analyses

Global Results

For descriptive purposes, shown in Table 1 are the average mean surface areas and mean depth for the STS_Ant and STS_Post regions in males and females, and between each rearing group. Heritability results on the combined sample showed the average surface area and mean depth of the STS_Ant and STS_Post regions were significantly heritable, while AQ values for both measures were not (see Table 2). With respect to average surface area and mean depth, scanner magnet was found to be a significant covariate, an expected finding, given the known differences in gray and white matter resolution as a function of field strength. Sex was also found to be a significant covariate, which was also expected, because we did not adjust for brain/body size between males and females (see Table 1). Neither age nor rearing history accounted for a significant proportion of variance in average surface area or mean depth. Also shown in Table 2 are the heritability results within the YNPRC and NCCC cohorts. Heritability in the surface areas were largely consistent between the two cohorts, but

this was not the case for the average depth measures for the STS_Ant and STS_Post measures.

Table 1: Average Mean Surface Area and Mean Depth (+/- s.e.) for the STS_Ant and STS_Post as a Function of Sex and Rearing History

	Sex			Rearing	
	Female	Male	MR	NR	WB
<i>Surface Area (mm²)</i>					
STS_Ant	1339.28 (19.54)	1483.65 (22.84)	1462.47 (22.09)	1419.75 (27.37)	1397.19 (42.63)
STS_Post	584.46 (13.35)	666.36 (15.60)	641.57 (15.09)	628.90 (18.69)	605.74 (29.11)
<i>Mean Depth (mm)</i>					
STS_Ant	11.57 (.094)	12.13 (.110)	12.02 (.106)	11.78 (.132)	11.76 (.205)
STS_Post	7.98 (.106)	7.94 (.124)	8.37 (.120)	8.08 (.148)	7.43 (.231)

Values in parentheses represent standard errors. MR = mother-reared, NR – nursery-reared, WB = wild-born. Surface area and mean depth are

Table 2: Heritability in STS_Ant and STS_Post Surface Area and Mean Depth for the Combined, YNPRC and NCCC Samples

	h^2	se	p	Covariates	Variance
<i>Combined Sample</i>					
Anterior Surface Area	.455	.123	.00003	Sc, Sex	.116
Posterior Surface Area	.316	.150	.0145	Sc, Sex	.135

Anterior Mean Depth	.345	.122	.0004	Sc, Sex	.083
Posterior Mean Depth	.183	.105	.0211	Sc, Rear	.027
YNPRC					
Anterior Surface Area	.501	.189	.003	Sc, Sex, Rear	.117
Posterior Surface Area	.356	.162	.005	Sc, Sex, Rear	.135
Anterior Mean Depth	.640	.205	.0004	Sc, Sex, Rear	.119
Posterior Mean Depth	.000	-----	.500	Sc	.016
NCCC					
Anterior Surface Area	.537	.154	.0003	Sc, Sex	.165
Posterior Surface Area	.660	.209	.0009	Sc, Sex	.091
Anterior Mean Depth	.000	-----	.500	Sc, Sex	.181
Posterior Mean Depth	.254	.143	.017	Sc, Sex	.068

se = standard error

We note here that surface area for the entire brain was significantly heritable ($h^2 = .298$, $se = .148$, $p = .011$). To determine whether the surface area heritability values for the STS were region specific or could be accounted for by overall surface area, we calculated the percentage of STS_Ant and STS_Post by dividing the mean surface areas for each area by the total surface area of the brain and multiplying by 100. We then re-ran the heritability analyses using the percentage STS_Ant and STS_Post measures with sex, age rearing and scanner as covariates. For both the STS_Ant ($h^2 = .325$, $se = .116$, $p = .0008$) and STS_Post ($h^2 = .223$, $se = .129$, $p = .033$) regions, the adjusted surface as measures remained significantly heritable. Thus, the heritability in

the STS surface area appears to be independent of genetic influences on total surface area.

Parameterized STS_Ant Depth

We next considered heritability in the STS_Ant depth measures at the 20 points along the anterior-posterior plane. Results for the average STS_Ant depth for the entire sample, as well as for the separate results for the NCCC and YNPRC cohorts, are shown in Figure 6a. For the combined sample, significant heritability was found for 13 of the 20 regions (regions 6 to 18); thus, the majority of regions along the anterior-posterior axis of the sulcus were significantly heritable with values ranging from .294 to .616. As with the global results and as expected, sex and scanner were significant covariates for 17 and 15 regions, respectively (see Table 3). Rearing was a significant covariate for regions 18 and 19 (see Table 3). The mean depth at the 20 STS regions for males and females and between the three rearing groups are shown in Table 4. As can be seen, when sex was a significant covariate, males had higher values than females. Further, for STS 18 and 19, MR apes had higher values than NR individuals who, in turn, had higher values than WB apes. Between the NCCC and YNPRC chimpanzee cohorts, the results were largely consistent, with significant heritability found in both the NCCC and YNPRC cohorts for STS regions 7 through 18 (see Figure 6b and 6c). For the AQ measures for each STS_Ant region, we found no evidence of significant heritability for any of the 20 STS regions, after adjustment for multiple comparisons, in either the combined sample or in each separate cohort.

Table 3: Heritability in STS_Ant Parameterized Regions and Variance Accounted for By Covariates

	h ²	s.e.	p	Covariates	Variance
STS1	.024	.106	.407	Sex	.015
STS2	.130	.107	.091	Sex, Scanner	.047
STS3	.175	.102	.025	Sex, Scanner	.078
STS4	.129	.106	.089	Sex, Scanner	.120
STS5	.129	.110	.098	Sex, scanner	.163
STS6	.294	.121	.002	Sex, Scanner	.124
STS7	.453	.127	.00002	Sex, Scanner	.163
STS8	.478	.132	.00001	Sex, Scanner	.158
STS9	.467	.131	.00002	Sec, Scanner	.152
STS10	.514	.129	.000007	Sex, Scanner	.157
STS11	.616	.118	.00000001	Sex, Scanner	.162
STS12	.482	.119	.00003	Sex, Scanner	.160
STS13	.499	.117	.000001	Sex, Scanner	.164
STS14	.604	.114	.0000001	Sex, Scanner	.154
STS15	.655	.119	.0000001	Sex, Scanner	.118
STS16	.501	.131	.00002	Sex, Scanner	.058
STS17	.482	.125	.0001	Sex	.032
STS18	.385	.137	.0009	Rear	.018
STS19	.105	.118	.159	Rear	.017
STS20	.000	.000	.500	None	

Table 4: Mean (+/- s.e.) STS Depth at the 20 STS locations as a Function of Sex and Rearing Group

	Sex		Rearing History		
	Male	Female	MR	NR	WB
STS1	4.93 (.089)	4.71 (.075)	4.74 (.085)	4.95 (.097)	4.87 (.156)
STS2	7.43 (.113)	7.06 (.095)	7.26 (.108)	7.37 (.123)	7.11 (.197)
STS3	8.90 (.119)	8.37 (.101)	8.75 (.114)	8.60 (.130)	8.55 (.208)
STS4	9.80 (.130)	9.28 (.110)	9.60 (.124)	9.46 (.142)	9.56 (.226)
STS5	10.46 (.135)	9.96 (.114)	10.19 (.129)	10.11 (.148)	10.34 (.236)

STS6	11.12 (.136)	10.63 (.115)	10.84 (.130)	10.76 (.149)	11.03 (.238)
STS7	11.89 (.131)	11.29 (.111)	11.59 (.125)	11.49 (.144)	11.71 (.229)
STS8	12.69 (.132)	12.01 (.111)	12.31 (.125)	12.19 (.144)	12.54 (.230)
STS9	13.40 (.131)	12.71 (.111)	13.01 (.125)	12.85 (.143)	13.30 (.229)
STS10	14.05 (.130)	13.31 (.110)	13.68 (.124)	13.48 (.142)	13.87 (.233)
STS11	14.62 (.131)	13.86 (.111)	14.34 (.125)	14.03 (.143)	14.34 (.228)
STS12	15.12 (.134)	14.31 (.113)	14.74 (.127)	14.48 (.146)	14.88 (.233)
STS13	15.48 (.139)	14.58 (.118)	15.08 (.133)	14.77 (.152)	15.24 (.243)
STS14	15.73 (.147)	14.82 (.124)	15.26 (.140)	15.03 (.160)	15.53 (.256)
STS15	16.05 (.161)	15.22 (.136)	15.58 (.154)	15.31 (.176)	16.03 (.282)
STS16	16.60 (.183)	15.95 (.155)	16.25 (.175)	15.91 (.200)	16.67 (.320)
STS17	16.91 (.200)	16.30 (.169)	16.75 (.191)	16.42 (.219)	16.64 (.350)
STS18	15.32 (.242)	14.76 (.204)	15.63 (.230)	15.09 (.264)	14.40 (.421)
STS19	11.31 (.223)	11.25 (.189)	11.81 (.213)	11.41 (.244)	10.63 (.390)
STS20	6.64 (.150)	6.75 (.127)	6.90 (.143)	6.76 (.164)	6.42 (.262)

Values in parentheses represent standard errors. MR = mother-reared, NR = nursery-reared, WB = wild-born.

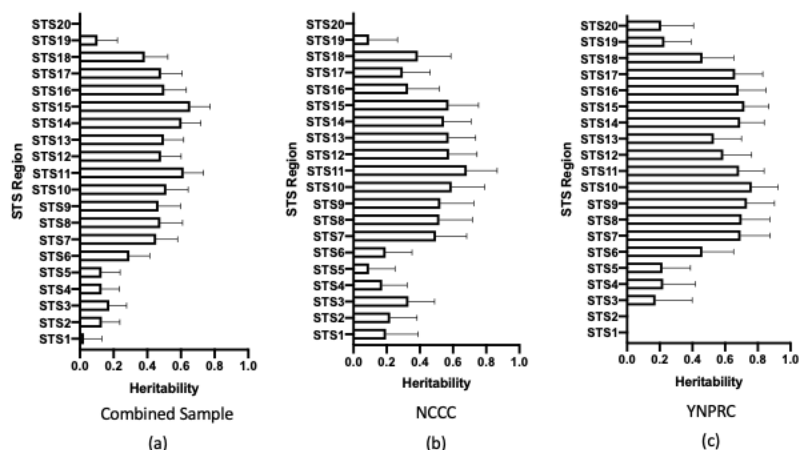


Figure 6: Heritability (+/- s.e.) for each of the 20 regions within the parameterized STS in the chimpanzees for the combined sample (a), NCCC (b) and YNPRC (c) samples.

Population-Level Asymmetry

Because LeRoy *et al.* (2015) emphasized the significance of asymmetries in the STAP as a uniquely human feature, we initially tested for population-level asymmetries in the global measures of the STS_Ant as well as its 20 antero-posterior depth measures in our sample. After adjustment to alpha using Bonferroni's correction procedure (adjusted $p = .002$), significant rightward asymmetries were found for STS regions 12 $t(290) = 3.555, p < .001$, 13 $t(290) = 4.065, p < .001$, 14 $t(290) = 4.183, p < .001$, 15 $t(290) = 3.863, p < .001$ and 16 $t(290) = 3.310, p < .001$ (see Figure 7). Separate one-sample t -tests within the NCCC and YNPRC cohorts revealed a consistent pattern of results (see Figure 8). For the NCCC sample, significant rightward asymmetries were found for STS 13 $t(157) = 2.201, p < .029$, 14 $t(157) = 2.598, p < .010$, 15 $t(157) = 2.873, p < .005$ and 16 $t(157) = 2.740, p < .007$. For the YNPRC sample, significant rightward asymmetries were found for STS regions 12 $t(128) =$

2.702, $p < .008$, 13 $t(128) = 3.21$, $p < .002$, 14 $t(128) = 3.068$, $p < .003$, and 15 $t(128) = 2.305$, $p < .023$. To test for rearing and sex effects, a MANCOVA was performed with the 20 STS regions serving as the dependent measures. No significant main effects or interactions were found.

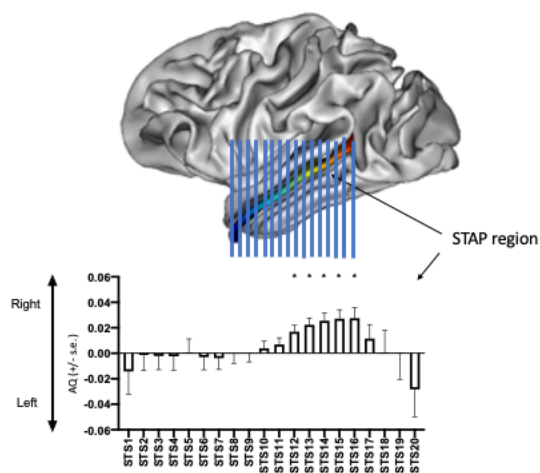


Figure 7: Upper panel: 3D rendering of chimpanzee brain with the STS_Ant region identified and that portion on which significant rightward asymmetries are evident. Lower panel: Mean AQ (+/- s.e.) scores for each of the 20 STS regions for the combined sample.

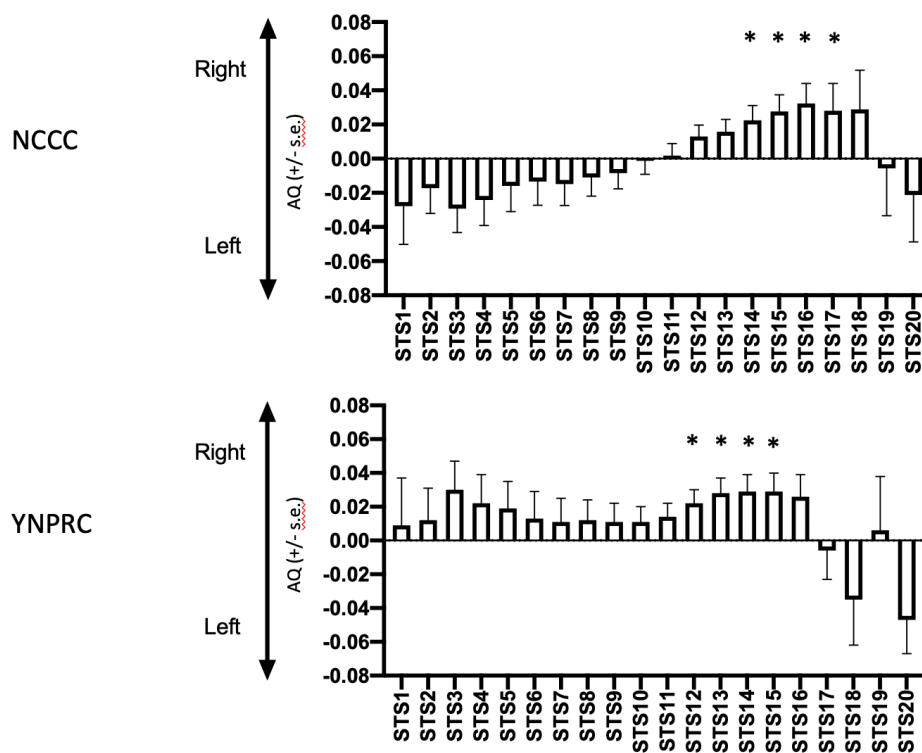


Figure 8: Mean AQ (+/- s.e.) scores for each of the 20 STS regions for the NCCC (upper panel) and YNPRC (lower panel) samples.

KIAA0319 SNPs and STS Morphology

Global

RS_P1: To test for the effect of the RS_P1 and RS_63 SNPs on STS_Ant and STS_Post, separate mixed model analyses of co-variance were performed with STS region as the repeated measure and genotype as between-group factors. Sex, rearing and scanner magnet were covariates. Further, because the STS measures were heritable, we also included the genetic relatedness score of each chimpanzee as an additional covariate. The genetic relatedness scores were based on the entire pedigree and reflected how related each chimpanzee subject was to all other individuals in the population. We found a significant main effect for RS_P1 genotype on average mean

depth $F(2, 242)=4.508$, $p = .012$, as well as a two-way interaction between STS region and genotype $F(2, 242)=7.179$, $p < .001$. Post-hoc analysis indicated that, for STS_Ant, average mean depth was significantly greater in chimpanzees with the AA compared to TT, but not the AT genotypes (see Table 5). In contrast, for the STS_Post, average mean depth was significantly higher in chimpanzees with the TT compared to AA, but not the AT genotypes (see Table 5). For the average surface area, as well as the AQ scores for the surface area and mean depth measure, we found no significant main effects or interactions for the RS_P1 genotypes.

Table 5: Descriptive Data for STS_Ant and STS_Post Average and Asymmetry Data for Chimpanzees with Different KIAA0319 Genotypes

RS_P1	Genotype		
	AA	AT	TT
<i>Surface Area</i>			
Mean STS_Ant	1441.56 (22.64)	1409.56 (21.74)	1389.87 (32.97)
Mean STS_Post	623.60 (15.34)	601.06 (14.73)	635.78 (22.34)
AQ STS_Ant	-0.011 (.014)	+0.040 (.014)	+0.013 (.021)
AQ STS_Post	-0.024 (.035)	-0.029 (.034)	-0.020 (.052)
<i>Mean Depth</i>			
Mean STS_Ant	12.05 (.108)	11.65 (.104)	11.69 (.158)
Mean STS_Post	7.95 (.122)	7.95 (.117)	8.72 (.177)
AQ STS_Ant	-0.006 (.009)	+0.010 (.009)	+0.013 (.014)
AQ STS_Post	-0.015 (.022)	-0.036 (.021)	-0.045 (.032)
RS_63	AA	AC	CC
<i>Surface Area</i>			

Mean STS_Ant	1454.34 (25.38)	1408.65 (21.05)	1382.29 (30.23)
Mean STS_Post	623.26 (17.52)	605.38 (14.53)	602.86 (20.87)
AQ STS_Ant	-0.006 (.016)	+0.018 (.013)	+0.027 (.019)
AQ STS_Post	+0.001 (.040)	-0.025 (.033)	-0.033 (.047)

Mean Depth

Mean STS_Ant	12.01 (.122)	11.69 (.101)	11.70 (.145)
Mean STS_Post	8.12 (.142)	8.03 (.118)	8.07 (.169)
AQ STS_Ant	+0.024 (.010)	-0.002 (.009)	-0.012 (.012)
AQ STS_Post	-0.035 (.025)	-0.020 (.021)	-0.029 (.030)

Bolded values indicated significant effect of KIAA0319 genotype. Values in parentheses represent standard errors.

RS_63: No significant main effects or interactions were found for this SNP.

STS_Ant Parameterization

To test for the effect of the RS_P1 and RS_63 SNPs on STS depth, separate mixed model analyses of co-variance were performed with STS region as the repeated measure and genotype as between-group factors. As above, genetic relatedness, sex, rearing and scanner magnet were covariates. For RS_P1, we found a significant main effect for genotype on average mean depth $F(2, 242) = 7.553, p = .021$ (see Figure 9a). Post hoc analysis indicated that chimpanzees with the AA allele had deeper folds than TT, but not AT individuals. No significant difference was found between chimpanzees with the AT and TT alleles. For the AQ values, we similarly found a main effect for genotype $F(2, 239) = 3.234, p = .041$ (see Figure 9b). Chimpanzees with the TT and AT genotypes showed significantly greater rightward asymmetries compared to the AA individuals. No significant difference was found in AQ scores for the chimpanzees with the AT and TT alleles. For RS_63 SNP, there were no significant main effects or interactions for either the average or AQ depth scores on the different alleles.

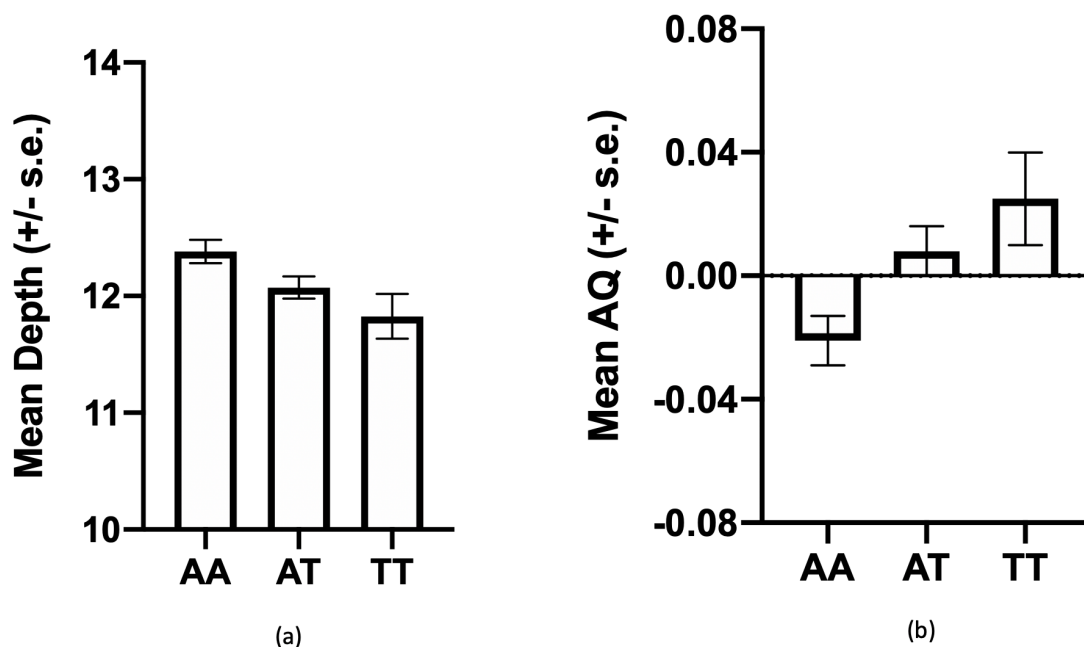


Figure 9: (a) Mean depth (+/- s.e.) and (b) Mean AQ (+/-s.e.) for chimpanzees with different polymorphism in RS_P1 in the KIAA0319 gene.

AVPR1A and STS Morphology

Global

A mixed model analysis of variance was performed on the *AVPR1A* gene with STS region as the repeated measure while genotype (DupB+/-, DupB-/) and sex served as between-group factors. Genetic relatedness, rearing history and scanner magnet were covariates. Separate analyses were performed for the average and AQ measures because they reflected different dimensions of STS morphology. There was a significant main effect for *AVP1A* genotype on average surface area $F(1, 232) = 4.407, p = .004$, but not average mean depth. DupB-/ chimpanzees had larger values than DupB+/-

apes (see Table 6). Regarding the AQ data, we found a significant main effect for *AVPR1A* genotype on surface area $F(1, 232) = 9.644, p < .001$ and mean depth $F(1, 232) = 7.127, p = .008$. For both measures, DupB^{-/-} chimpanzees had greater rightward asymmetries than DupB^{+/-} apes (see Figure 10a and 10b).

Table 6: Descriptive Data for STS_Ant and STS_Post Average and Asymmetry Data for Chimpanzees with Different *AVPR1A* Genotypes

AVPR1A	Genotype	
	DupB ^{-/-}	DupB ^{+/-}
<i>Surface Area</i>		
Mean STS_Ant	1440.81 (17.99)	1377.85 (23.91)
Mean STS_Post	606.90 (12.97)	604.45 (17.25)
AQ STS_Ant	+0.030 (.012)	+0.014 (.015)
AQ STS_Post	-0.007 (.030)	-0.102 (.039)
<i>Mean Depth</i>		
Mean STS_Ant	11.90 (.085)	11.65 (.112)
Mean STS_Post	7.88 (.100)	8.25 (.133)
<i>AQ STS_Ant</i>	<i>+0.009 (.007)</i>	<i>+0.006 (.010)</i>
<i>AQ STS_Post</i>	<i>-0.011 (.019)</i>	<i>-0.085 (.025)</i>

Bolded values indicated significant effect of *AVPR1A* genotype. *Italicized* values indicate significant interaction between STS region and *AVPR1A* genotype. Values in parentheses represent standard errors.

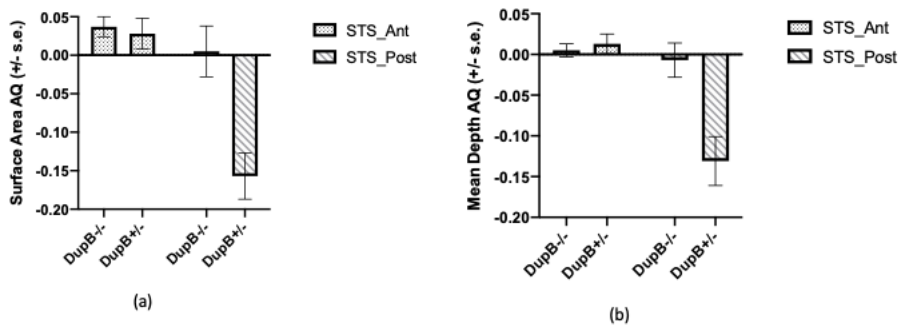


Figure 10: Mean surface area AQ (+/- s.e.) (a) and Mean depth AQ (+/- s.e.) (b) for the STS_Ant and STS_Post measures in chimpanzees with different alleles for the AVPR1A gene.

STS Parameterization

A mixed model analysis of variance was performed on the *AVPR1A* gene with STS region as the repeated measure while genotype (DupB+/-, DupB-/-) and sex served as between-group factors. Genetic relatedness, rearing history and scanner magnet were covariates. For the average depth measures, a significant main effect for *AVPR1A* genotype was found $F(1, 234) = 7.602, p = .006$, as well as a two-way interaction between *AVPR1A* and STS region $F(19, 4446) = 1.747, p = .023$. For the *AVPR1A* genotype by STS region interaction, post-hoc analysis indicated that DupB-/- apes had greater mean depth values than DupB+/- individuals for regions 7 through 19 (see Figure 11, left panel). Regarding STS asymmetry, the analysis revealed a significant two-way interaction between *AVPR1A* genotype and STS region $F(19, 4446) = 2.378, p < .001$ (Figure 11, right panel). For regions 12, 13, 14 and 18, post-hoc analysis indicated that DupB-/- apes had greater rightward asymmetries than Dup+/-

apes. By contrast, DupB^{-/-} apes had greater leftward asymmetries than DupB^{+/-} apes for region 3.

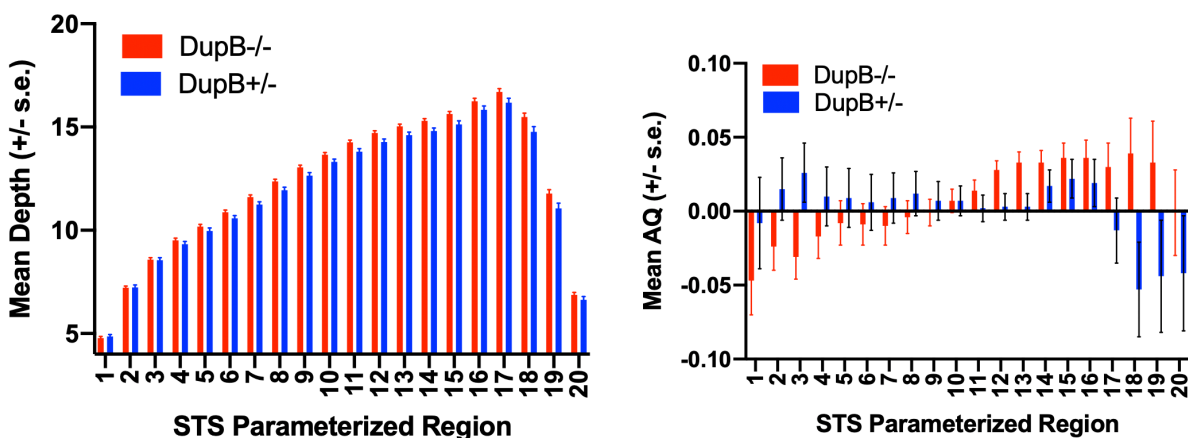


Figure 11: Mean depth (+/- s.e.) (left panel) and Mean AQ (+/-s.e.) (right panel) for chimpanzees with different AVPR1A alleles within the parameterized STS_Ant region.

Effect of KIAA0319 & AVPR1A on Central Sulcus (CS) Surface Area and Depth

In this final analysis, we tested for the influence of the KIAA0319 and AVPR1A SNPs on the surface area and depth of the CS. The details for extraction, labeling and parameterization of the CS were identical to those used for the STS and have been described in detail elsewhere (REFS). The only major difference was in the parameterization direction which was performed along the superior-inferior plane for the CS as opposed to the anterior-posterior plane for the STS. As with the STS, depth of the CS was measured at 100 sulcal length positions in an superior-to-inferior progression along the parameterized sulcal mesh surface. Position 1 was located at the most superior point of CS while position 100 was located at the most inferior point of the CS. As with the STS, to simplify the analyses, within the left and right hemispheres, we averaged every 5 depth measures from point 0 to 100 to create 20 CS regions along the

anterior-posterior plane. We also computed AQ values at each of the 20 CS regions following the formula described above for the STS.

Global Measures

In the initial analysis, we tested whether the influence of polymorphisms in the KIAA0319 and AVPR1A genes influenced the average surface area (CS_ASA), average mean depth (CS_AMD), overall surface area AQ (CSSA_AQ) and overall mean depth AQ (CSMD_AQ) values of the CS. To test for the effect of the RS_P1 and RS_63 SNPs on these 4 CS measures, multiple analyses of covariance (MANCOVA) was performed with CS_ASA, CS_AMD, CSSA_AQ and CSMD_AQ as dependent measures while sex and genotype were between-group factors. Rearing, scanner magnet and relatedness coefficients were covariates. No significant main effect or interactions were found for either of the KIAA0319 SNP polymorphisms. With respect to AVPR1A, the MANCOVA revealed a significant main effect for AVPR1A $F(4, 228) = 2.575, p = .03$. Subsequent univariate F -test revealed a significant effect for the CSMD_AQ values. DupB^{-/-} individuals had greater rightward asymmetry values compared to DupB^{+/-} apes (see Table 7).

Table 7: Mean CS_ASA, CS_AMD, CSSA_AQ and CSMD_AQ Values (+/- s.e.) for Chimpanzee with Different KIAA0319 and AVPR1A Genotypes

	CS_ASA	CS_AMD	CSSA_AQ	CSDM_AQ
<i>KIAA0319</i>				
<i>RS_P1</i>				
AA	1544.58 (19.87)	9.32 (.073)	+0.002 (.014)	+0.001 (.010)
AT	1493.76 (19.57)	9.24 (.071)	+0.019 (.013)	-0.003 (.010)
TT	1544.00	9.56	+0.002	-0.007

	(29.09)	(.106)	(.020)	(.014)
RS_63				
AA	1551.75 (23.29)	9.35 (.085)	+0.014 (.016)	-0.015 (.011)
AC	1512.40 (18.47)	9.23 (.067)	+0.019 (.012)	+0.003 (.009)
CC	1491.11 (28.59)	9.26 (.10)	-0.008 (.019)	+0.004 (.014)
AVPR1A				
DupB-/-	1542.87 (17.09)	9.38 (.063)	+0.016 (.014)	+0.008 (.008)
DupB+/-	1498.25 (22.41)	9.19 (.082)	-0.012 (.014)	-0.018 (.010)

Bolded values indicated significant effect of AVPR1A genotype. Values in parentheses represent standard errors.

CS Parameterization

For these analyses, the mean depth and AQ values at the 20 CS locations were the repeated measures while sex and genotype were the between group factors. Rearing, scanner and genetic relatedness were the covariates. Regarding KIAA0319, we found no significant main effects or interactions for RS_P1 nor RS-63 on either average depth or the depth AQ values. By contrast, for the AVPR1A genotypes, we found a significant main effects for genotype on the AQ score $F(1, 237) = 4.002, p = .047$. DupB-/- apes had significantly greater rightward asymmetry values (*Mean AQ* = .128, *s.e.* = .075) compared to DupB+/- (*Mean AQ* = -.123, *s.e.* = .100) chimpanzees.

Discussion

The results of this study are straightforward. First, the surface area and depth of the STS, particularly in the central portions, were found to be significantly heritable and

these findings were consistent between the NCCC and YNPRC cohorts of chimpanzees. Second, and consistent with the previous report by LeRoy et al. (2015), chimpanzees show a small, but nonetheless significant, population-level rightward asymmetry in the STAP region within the STS. Lastly, one SNP within the *KIAA0319* gene was found to have a significant impact on the depth and asymmetry in the STAP regions within the STS. Similarly, an indel deletion with the arginine vasopressin receptor 1A gene, *AVPR1A*, was found to be associated with both the mean depth and asymmetry within the STS.

Regarding the results on lateralization, the significant rightward asymmetries in the STAP region are of interest for two reasons. First, as we have reported for measures of the planum temporale in chimpanzees (Spocter *et al.* 2020), the findings were largely consistent between the NCCC and YNPRC cohorts of captive chimpanzees suggesting that this bias is repeatable in at least two genetically isolated populations of apes. Second, the STS was quantified slightly differently than the method used by LeRoy et al. (2015). Therefore, it also appears that the small but significant rightward asymmetries in the STAP region are evident independent of the methods used to quantify it. More generally, the overall significant rightward asymmetries in the STAP region clearly challenge the claim that these asymmetries are uniquely human, though admittedly, the magnitude of the bias is decidedly smaller in chimpanzees compared to humans. We also note that significant rightward asymmetries have been reported in the overall surface area of the STS in macaques (Bogart et al. 2012; Suwada 2020), though it is unclear if these effects are attributable to lateralization within the STAP region because these previous studies did not delineate

the STS in the manner that was utilized in this report. Future studies in other species should seek to clarify the nature of STS asymmetry in the context of the location of STAP region.

We also found that the overall surface area, overall mean depth and the mean depth for the majority of STS depth regions were significantly heritable. Further, heritability results were similar between the NCCC and YNPRC samples, suggesting that the contributions of genetic factors to individual variation in STS morphology are consistent and repeatable. The evidence of consistent and repeatable heritability in the STS is not surprising, in some ways, because the STS is a conserved fold that evolved early in primate brain evolution (Zilles et al. 1989; Gilissen 1992; Sawada et al. 2010) and, ontogenetically, emerges during embryonic development in human and nonhuman primates (White et al. 2010; Habas et al. 2012; Meng et al. 2018). More evolutionary conserved sulci have been found to be more strongly heritable in humans and chimpanzees (Gomez-Robles et al. 2015) and our findings on the STS appear to be consistent with these previous results. It is of further note that the heritability in the overall surface area and depth of the STS in our chimpanzee sample are within the range of values reported in humans in a recent paper by Pizzagalli et al. (2020) who similarly used BrainVisa to quantify the STS (and many other sulci).

We failed to find any evidence whatsoever that asymmetries in the STS were significantly heritable, a finding consistent with previous results for sulci within the inferior frontal gyrus (Hopkins, Misiura, et al. 2015) and central sulcus (Hopkins, Coulon, Meguerditchian, Autrey, Davidek, Mahovetz, S., *et al.* 2017) of chimpanzees. This implies that there are no genes that specifically code for left-right difference in surface

area and depth within the STS and other sulci of the chimpanzee cerebral cortex. Some have hypothesized that one evolutionary shift that occurred in brain organization after the split between chimpanzees and humans from their common ancestor was a genetic basis for the expression of population-level lateralization in structure and function (Warren 1980; Annett 2002; Crow 2009; Corballis et al. 2012). The results reported here are consistent with this view, at least as it pertains to a lack of evidence for a genetic basis for asymmetries in the STS of chimpanzees. However, there are at least two caveats to this conclusion. First, recall that we found that polymorphisms in the RS_P1 SNP of the *KIAA0319* gene and the indel deletion of the *AVPR1A* gene were associated with asymmetries in the overall anterior portion of the STS. Thus, though AQ values were not heritable, at least one SNP in the *KIAA0319* and a deletion in the *AVPR1A* gene were associated with variation in the AQ values which would suggest a genetic basis for STS asymmetry. Second, it is worth noting that the evidence for a genetic basis in determining directional asymmetries in humans is not terribly robust (Armour et al. 2014; Pletikos et al. 2014; Carrion-Castillo et al. 2019; de Kovel and Francks 2019; Schmitz et al. 2019; Carrion-Castillo et al. 2020; Sha et al. 2021) and certainly does not support single or dual allele models of asymmetry that have been postulated in previous genetic models of behavioral and brain asymmetry. In short, the role of genetic factors on the determination of population-level structural and functional asymmetries remains unclear but merits further investigation (Ocklenburg and Gunturkun 2018; Schmitz *et al.* 2019).

In our view, the overall findings of this study support the view of Redcay (2008) with respect to the diverse roles and function that are subserved by the STS, particularly

in the context of the role of the *KIAA0319* and *AVPR1A* genes on behavior.

Specifically, Redcay (2008) has suggested that the STS plays a fundamental role in the processing of visual and auditory sequential information and interpreting the meaning or communicative function of these stimuli. This general neural processing principle would apply to a broad range of stimuli and arguably across species but particularly among other closely-related primate species such as chimpanzees. For instance, chimpanzee communication is multimodal and involves the processing and integration of facial, vocal and gestural signals. Within this framework, the computational need to interpret these sequential, multimodal signals might explain why polymorphisms in purported language genes, such as *KIAA0319*, would have anatomical consequences on STS morphology in species that lack full-blown language.

The potential specificity of the role of *KIAA0319* and *AVPR1A* on STS morphology is further supported by the findings (or lack thereof) of the effect of the polymorphisms for each these genes on variation in the CS. Notably, neither of SNPs for the *KIAA0319* gene had a significant effect on CS surface area, mean depth or asymmetries in these measures. A significant main effect for *AVPR1A* was found for the overall CS depth asymmetry values with DupB/- individuals showing greater rightward asymmetries. This pattern in directional asymmetry is similar to the findings reported for the STS_ant parameterization results; however, the influence of the *AVPR1A* polymorphisms were specific to the posterior regions and not the entire fold as was the case for the CS. Therefore, interpreting the collective effect of *AVPR1A* on asymmetries in sulci surface area and depth is not straight forward. Conservatively, when comparing the overall influence of these genes on sulci surface area and depth,

our findings suggest a more region-specific impact of *KIAA0319* on STS morphology and asymmetry compared to *AVPR1A*.

In summary, we found that chimpanzees show a small but significant rightward asymmetry in the STAP region within the STS. Additionally, the surface area and depth of the STS was found to be significantly heritable and these results were repeatable in two genetically isolated populations of chimpanzees. Asymmetries in the surface area and depth of the STS were not found to be significantly heritable. Single nucleotide polymorphisms in two genes, *KIAA0319* and *AVPR1A*, were also found to be associated with individual variation in the depth of the STS. Collectively, the data provide new insights into factors that influence individual variation and evolution of STS morphology in hominids.

Acknowledgement

This work was supported, in part, by NIH grants AG-067419, NS-073134, NS-42867, and NS-092988. Chimpanzee maintenance at the National Center for Chimpanzee Care was previously funded by NIH/NCRR U42- OD-011197. For portions of this work, W.D.H. was also supported by (1) the IMERA/ILCB residency program (ANR-16-CONV-0002) of Aix-Marseille Universite and its Excellence Initiative (A*MIDEX) and (2) the Blaise-Pascal Chair of Region Ile de France and Université Paris-Saclay. A.M has received funding from the European Research Council under the European Union's Horizon 2020 research and innovation program grant agreement No 716931 - GESTIMAGE - ERC-2016-STG. All aspects of this research conformed to existing US and NIH federal policies on the ethical use of chimpanzees in research. Reprint requests may be sent to: William D Hopkins, Department of Comparative Medicine, Keeling Center for Comparative Medicine and Research, Bastrop, Texas 78602 Email: wdhopkins@mdanderson.org

References

- Almasy L, Blangero J. 1998. Multipoint quantitative-trait linkage analysis in general pedigrees. *American Journal of Human Genetics*. 62:1198-1211.
- Anestis SF, Webster TH, Kamilar JM, Fontenot MB, Watts DP, Bradley BJ. 2014. AVPR1A variation in chimpanzees (*Pan troglodytes*): Population differences and association with behavioral style. *International Journal of Primatology*. 35:305-324.
- Annett M. 2002. *Handedness and brain asymmetry: The right shift theory*. Hove: Psychology Press.
- Armour JAL, Davison A, McManus IC. 2014. Genome-wide association study of handedness excludes simple genetic models. *Heredity*. 112:221-225.
- Bailey P, von Bonin G, McCulloch WS. 1950. *The isocortex of the chimpanzee*. Urbana-Champaign: University of Illinois Press.
- Bard KA. 1994. Evolutionary roots of intuitive parenting: Maternal competence in chimpanzees. *Early Development and Parenting*. 3:19-28.
- Bard KA, Platzman KA, Lester BM, Suomi SJ. 1992. Orientation to social and nonsocial stimuli in neonatal chimpanzees and humans. *Infant Behavior and Development*. 15:43-56.
- Bodin C, Pron A, Le Mao M, Regis J, Belin P, Coulon O. 2021. Plis de passage in the superior temporal sulcus: Morphology and local connectivity. *Neuroimage*. 225:117513.
- Bogart SL, Bennett AJ, Schapiro SJ, Reamer LA, Hopkins WD. 2014. Different early rearing experiences have long term effects on cortical organization in captive chimpanzees (*Pan troglodytes*) *Developmental Science*. 17:161-174.

- Bogart SL, Mangin JF, Schapiro SJ, Reamer L, Bennett AJ, Pierre PJ, Hopkins WD. 2012. Cortical sulci asymmetries in chimpanzees and macaques: A new look at an old idea. *Neuroimage*. 61:533-541.
- Brakke KE, Savage-Rumbaugh ES. 1995. The development of language skills in bonobo and chimpanzee - i. comprehension. *Language and Communication*. 15:121-148.
- Brakke KE, Savage-Rumbaugh ES. 1996. The development of language skills in *Pan* - ii. production. *Language and Communication*. 16:361-380.
- Carrion-Castillo A, Pepe A, Kong XZ, Fisher SE, Mazoyer B, Tzourio-Mazoyer N, Crivello F, Francks C. 2020. Genetic effects on planum temporale asymmetry and their limited relevance to neurodevelopmental disorders, intelligence or educational attainment. *Cortex*. 124:137-153.
- Carrion-Castillo A, Van der Haegen L, Tzourio-Mazoyer N, Kavaklioglu T, Badillo S, Chavent M, Saracco J, Brysbaert M, Fisher SE, Mazoyer B, Francks C. 2019. Genome sequencing for rightward hemispheric language dominance. *Genes Brain Behav*. 18:e12572.
- Carter CS. 2007. Sex differences in oxytocin and vasopressin: Implications for autism spectrum disorders? *Behavioral Brain Research*. 176:170-186.
- Connolly CJ. 1936. The fissural pattern of the primate brain. *American Journal of Physical Anthropology*. 11:31-421.
- Connolly CJ. 1950. External morphology of the primate brain. Springfield, Illinois: Charles C Thomas Publisher.

Cope N, Harold D, Hill G, Moskvina V, Stevenson JL, Holmans P, Owen MJ, O'Donovan MC, Williams J. 2005. Strong evidence that KIAA0319 on chromosome 6p is a susceptibility gene for developmental dyslexia. *American Journal of Human Genetics*. 76:581-591.

Corballis MC, Badzakova-Trajkov G, Haberling IS. 2012. Right hand, left brain: genetic and evolutionary basis of cerebral asymmetries for language and manual action. *WIREs Cognitive Science*. 3:1-17.

Coulon O, Lefevre J, Kloppel S, Siebner H, Mangin JF editors. Quasi-isometric length parameterization of cortical sulci: application to handedness and the central sulcus morphology, 12th IEEE International Symposium on Biomedical imaging; 2015; Brooklyn, New York

Coupe P, Yger P, Prima S, Hellier P, Kervrann C, Barillot C. 2008. An optimized blockwise nonlocal means denoising filter for 3-D magnetic resonance images. *IEEE Trans Med Imaging*. 27:425-441.

Crow TJ. 2009. A theory of the origin of cerebral asymmetry: Epigenetic variation superimposed on a fixed right-shift Laterality. 15:289-303.

Darki F, Peyrard M, Matsson H, Kere J, Klingberg T. 2012. Three dyslexia susceptibility genes, DYX1C1, DCDC2, and KIAA0319, affect temporo-parietal white matter structure. *Biological Psychiatry*. 72:671-676.

de Kovel CGF, Francks C. 2019. The molecular genetics of hand preference revisited. *Sci Rep*. 9:5986.

Deen B, Koldewyn K, Kanwisher N, Saxe R. 2015. Functional Organization of Social Perception and Cognition in the Superior Temporal Sulcus. *Cereb Cortex*. 25:4596-4609.

Dennis MY, Paracchini S, Scerri TS, Prokunina-Olsson L, Knight JC, Wade-Martins R, Coghill P, Beck S, Green ED, Monaco AP. 2009. A common variant associated with dyslexia deduces expression of the KIAA0319 gene. *PLoS Genetics*. 5:e1000436.

Donaldson ZR, Bai Y, Kondrashov FA, Stoinski TL, Hammock EAD, Young LJ. 2008. Evolution of a behavior-linked microsatellite-containing element of the 5' flanking region of the primate *avpr1a* gene *BMC Evolutionary Biology*. 8:180-188.

Donaldson ZR, Young LJ. 2008. Oxytocin, vasopressin and the neurogenetics of sociality. *Science*. 322:900-904.

Eckert MA, Berninger VW, Vaden KI, Jr., Gebregziabher M, Tsu L. 2016. Gray Matter Features of Reading Disability: A Combined Meta-Analytic and Direct Analysis Approach(1,2,3,4). *eNeuro*. 3.

Eicher JD, Montgomery AM, Akshoomoff N, Amaral DG, Bloss CS, Libiger O, Schork NJ, Darst BF, Casey BJ, Chang L, Ernst T, Frazier J, Kaufmann WE, Keating B, Kenet T, Kennedy D, Mostofsky S, Murray SS, Sowell ER, Bartsch H, Kuperman JM, Brown TT, Hagler DJ, Jr., Dale AM, Jernigan TL, Gruen JR, Pediatric Imaging Neurocognition Genetics S. 2016. Dyslexia and language impairment associated genetic markers influence cortical thickness and white matter in typically developing children. *Brain Imaging Behav*. 10:272-282.

Fears SC, Melega WP, Service SK, Lee C, Chen K, Tu Z, Jorgensen MJ, Fairbanks LA, Cantor RM, Freimer NB, Woods RP. 2009. Identifying heritable brain phenotypes in an extended pedigree of vervet monkeys. *The Journal of Neuroscience*. 29:2867-2875.

Fears SC, Scheibel K, Abaryan Z, Lee C, Service SK, Jorgensen MJ, Fairbanks LA, Cantor RM, Freimer NB, Woods RP. 2011. Anatomic brain asymmetry in vervet monkeys. *PlosOne*. 6:e28243.

Francis SM, Kistner-Griffin E, Yan Z, Guter S, Cook EH, Jacob S. 2016. Variants in Adjacent Oxytocin/Vasopressin Gene Region and Associations with ASD Diagnosis and Other Autism Related Endophenotypes. *Front Neurosci*. 10:195.

French JA, Taylor JH, Mustoe AC, Cavanaugh J. 2016. Neuropeptide diversity and the regulation of social behavior in New World primates. *Front Neuroendocrinol*. 42:18-39.

Gilissen E. 1992. The neocortical sulci of the capuchin monkey (*Cebus*): evidence for asymmetry in the sylvian sulcus and comparison with other primates. *Comptes Rendus de l'Academie de Sciences Paris, Series III*. 314:165-170.

Gomez-Robles A, Hopkins WD, Schapiro SJ, Sherwood CC. 2015. Relaxed genetic control of cortical organization in human brains compared with chimpanzees. *Proc Natl Acad Sci U S A*. 112:14799-14804.

Goodson JL, Bass AH. 2001. Social behavior functions and related anatomical characteristics of vasotocin/vasopressin systems in vertebrates. *Brain Research Reviews*. 35:246-265.

Habas PA, Scott JA, Roosta A, Rajagopalan V, Kim K, Rousseau F, Barkovich AJ, Glenn OA, Studholme C. 2012. Early folding patterns and asymmetries of the normal human brain detected from in utero MRI. *Cereb Cortex*. 22:13-25.

Hammock EA, & Young, L.J. 2005. Microsatellite instability generates diversity in brain and sociobehavioral traits. *Science*. 308:1630-1634.

Hammock EA, Young LJ. 2006. Oxytocin, vasopressin and pair bonding: implications for autism. *Philosophical Transactions of the Royal Society of London Series B, Biological Sciences*. 361:2187-2198.

Hopkins WD, Coulon O, Mangin JF. 2010. Observer-independent characterization of sulcal landmarks and depth asymmetry in the central sulcus of the chimpanzee brain. *Neuroscience* 171:544-551.

Hopkins WD, Coulon O, Meguerditchian A, Autrey M, Davidek K, Mahovetz L, Pope S, Mareno MC, Schapiro SJ. 2017. Genetic factors and orofacial motor learning selectively influence variability in central sulcus morphology in chimpanzees (*Pan troglodytes*). *J Neurosci*. 37:5475-5483.

Hopkins WD, Coulon O, Meguerditchian A, Autrey MM, Davidek K, Mahovetz LM, S. P, Mareno MC, Schapiro SJ. 2017. Genetic factors and oro-facial motor learning selectively influence variability in central sulcus morphology in chimpanzees (*Pan troglodytes*). *J Neurosci*. 37:5475-5483.

Hopkins WD, Donaldson ZR, Young LY. 2012. A polymorphic indel containing the RS3 microsatellite in the 5' flanking region of the vasopressin V1a receptor gene is associated with chimpanzee (*Pan troglodytes*) personality. *Genes, Brain and Behavior*. 11:552-558.

Hopkins WD, Keebaugh AC, Reamer LA, Schaeffer J, Schapiro SJ, Young LJ. 2014. Genetic influences on receptive joint attention in chimpanzees (*Pan troglodytes*). *Scientific Reports* 4:1-7.

Hopkins WD, Latzman RD. 2021. Role of Oxytocin and Vasopressin V1a Receptor Variation on Personality, Social Behavior, Social Cognition, and the Brain in Nonhuman Primates with a Specific Emphasis in Chimpanzees. In: Wilczynski W, Brosnan SF, editors. *Social Cooperation and Conflict: Biological Mechanisms at the Interface* New York: Cambridge University Press p 134-160.

Hopkins WD, Latzman RD, Marenco MC, Schapiro SJ, Gomez-Robles A, Sherwood CC. 2018. Heritability of Gray Matter Structural Covariation and Tool Use Skills in Chimpanzees (*Pan troglodytes*): A Source-Based Morphometry and Quantitative Genetic Analysis. *Cerebral Cortex*.

Hopkins WD, Marenco MC, Schapiro SJ. 2019. Further evidence of left hemisphere dominance in motor skill by chimpanzees on a tool use task. *Journal of Comparative Psychology*. 133:512-519.

Hopkins WD, Meguerditchian A, Coulon O, Bogart SL, Mangin JF, Sherwood CC, Grabowski MW, Bennett AJ, Pierre PJ, Fears SC, Woods RP, Hof PR, Vauclair J. 2014. Evolution of the central sulcus morphology in primates. *Brain, Behavior and Evolution*. 84:1930.

Hopkins WD, Misiura M, Pope SM, Latash EM. 2015. Behavioral and brain asymmetries in primates: A preliminary evaluation of two evolutionary hypotheses. *Yearbook of Cognitive Neuroscience*. 1359:65-83.

Hopkins WD, Misiura M, Reamer LA, Schaeffer JA, Marenco MC, Schapiro SJ. 2014. Poor receptive joint attention skills are associated with atypical grey matter asymmetry in the posterior superior temporal gyrus of chimpanzees (*Pan troglodytes*). *Frontiers in Cognition*. 5:1-8.

Hopkins WD, Nir T. 2010. Planum temporale surface area and grey matter asymmetries in chimpanzees (*Pan troglodytes*): The effect of handedness and comparison within findings in humans. *Behavioural Brain Research* 208:436-443.

Hopkins WD, Reamer L, Mareno MC, Schapiro SJ. 2015. Genetic basis for motor skill and hand preference for tool use in chimpanzees (*Pan troglodytes*). *Proceedings of the Royal Society: Biological Sciences* B. 282.

Hopkins WD, Staes N, Mulholland MM, Schapiro SJ, Rosenstein M, Stimpson C, Bradley BJ, Sherwood CC. 2021. Gray Matter Variation in the Posterior Superior Temporal Gyrus Is Associated with Polymorphisms in the KIAA0319 Gene in Chimpanzees (*Pan troglodytes*). *eNeuro*. 8.

Hopkins WD, Staes N, Mulholland MM, Schapiro SJ, Rosenstein M, Stimpson CD, Bradey BJ, sherwood CC. in press. Gray matter variation in the posterior superior temporal gyrus is associated with polymorphisms in the KIAA0319 gene in chimpanzees (*Pan troglodytes*). *eNeuro*.

Kong XZ, Mathias SR, Guadalupe T, Group ELW, Glahn DC, Franke B, Crivello F, Tzourio-Mazoyer N, Fisher SE, Thompson PM, Francks C. 2018. Mapping cortical brain asymmetry in 17,141 healthy individuals worldwide via the ENIGMA Consortium. *Proc Natl Acad Sci U S A*.

Latzman RD, Hopkins WD, Keebaugh AC, Young LJ. 2014. Personality in chimpanzees (*Pan troglodytes*): Exploring the hierarchical structure and associations with the vasopressin V1A receptor gene. *PLoS One*. 9:e95741.

Le Guen Y, Leroy F, Auzias G, Riviere D, Grigis A, Mangin JF, Coulon O, Dehaene-Lambertz G, Frouin V. 2018. The chaotic morphology of the left superior temporal sulcus is genetically constrained. *Neuroimage*. 174:297-307.

LeRoy F, Cai Q, Bogart SL, Dubois J, Coulon O, Monzalvo K, Fischer C, Glasel H, Van der Haegen L, Benezit A, Lin CP, Kennedy DN, Ihara AS, Hertz-Pannier L, Moutard ML, Poupon C, Brysbaert M, Roberts N, Hopkins WD, Mangin JF, Dehaene-Lambertz G. 2015. New human-specific brain landmark: The depth asymmetry of superior temporal sulcus. *Proceedings of the National Academy of Sciences*.

Mahovetz LM, Young LJ, Hopkins WD. 2016. The influence of AVPR1A genotype on individual differences in behaviors during a mirror self-recognition task in chimpanzees (*Pan troglodytes*). *Genes Brain Behav*. 15:445-452.

Mangin JF editor. Entropy minimization for automatic correction of intensity nonuniformity, MMBIA; 2000; Hilton Head, South Carolina:IEEE Press. 162-169 p.

Mangin JF, Riviere D, Cachia A, Duchesnay E, Cointepas Y, Papadopoulos-Orfanos D, Collins DL, Evans AC, Regis J. 2004. Object-based morphometry of the cerebral cortex. *Medical Imaging*. 23:968-982.

McKay DR, Kochunov PV, Cykowski MD, Kent JW, Laird AR, Lancaster JL, Blangero J, Glahn DC, Fox PT. 2013. Sulcus depth-position profile is a genetically mediated neuroscientific trait; Description and characterization in the central sulcus. *The Journal of Neuroscience*. 33:15618-15625.

Melke J. 2008. Autism: Which genes are involved? . *Clinical Neuropsychiatry*. 5:63-69.

Meng Y, Li G, Wang L, Lin W, Gilmore JH, Shen D. 2018. Discovering cortical sulcal folding patterns in neonates using large-scale dataset. *Hum Brain Mapp*. 39:3625-3635.

- Mulholland MM, Navabpour S, Mareno MC, Schapiro SJ, Young LY, Hopkins WD. 2020. AVPR1A variation is linked to gray matter covariation in the social brain network of chimpanzees. *Genes, Brain and Behavior*. 19:e12631.
- Mundy P. 2018. A review of joint attention and social-cognitive brain systems in typical development and autism spectrum disorder. *Eur J Neurosci*. 47:497-514.
- Ocklenburg S, Gunturkun O. 2018. *The Lateralized Brain: The Neuroscience and Evolution of Hemispheric Asymmetries*. London: Academic Press.
- Parker KJ, Garner JP, Oztan O, Tarara ER, Li J, Sclafani V, Del Rosso LA, Chun K, Berquist SW, Chez MG, Partap S, Hardan AY, Sherr EH, Capitanio JP. 2018. Arginine vasopressin in cerebrospinal fluid is a marker of sociality in nonhuman primates. *Sci Transl Med*. 10.
- Pinel P, Fauchereau F, Moreno A, Barbot A, Lathrop M, Zelenika D, Le Bihan D, Poline J-B, Bourgeron T, Dehaene S. 2012. Genetic variants of FOXP2 and KIAA0319/TTRAP/THEM2 locus are associated with altered brain activation in distinct language-related regions. *J Neurosci*. 32:817-825.
- Pizzagalli F, Auzias G, Yang Q, Mathias SR, Faskowitz J, Boyd JD, Amini A, Riviere D, McMahon KL, de Zubicaray GI, Martin NG, Mangin JF, Glahn DC, Blangero J, Wright MJ, Thompson PM, Kochunov P, Jahanshad N. 2020. The reliability and heritability of cortical folds and their genetic correlations across hemispheres. *Commun Biol*. 3:510.
- Plaze M, Paillere-Martinot ML, Penttila J, Januel D, de Beaurepaire R, Bellivier F, Andoh J, Galinowski A, Gallarda T, Artiges E, Olie JP, Mangin JF, Martinot JL, Cachia A. 2011. "Where do auditory hallucinations come from?"--a brain morphometry study of

schizophrenia patients with inner or outer space hallucinations. *Schizophr Bull.* 37:212-221.

Pletikos M, Sousa AMM, Sedmak G, Meyer KA, Zhu Y, Cheng F, Li M, Kawasawa YI, Sestan N. 2014. Temporal specification and bilaterality of human neocortical topographic gene expression. *Neuron.* 81.

Redcay E. 2008. The superior temporal sulcus performs a common function for social and speech perception: implications for the emergence of autism. *Neurosci Biobehav Rev.* 32:123-142.

Robichon F, Levrier O, Farnarier P, Habib M. 2000. Developmental dyslexia: atypical cortical asymmetries and functional significance. *European Journal of Neurology.* 7:35-46.

Rogers J, Kochunov PV, Lancaster JL, Sheeedy W, Glahn D, Blangero J, Fox PT. 2007. Heritability of brain volume, surface area and shape: An MRI study in an extended pedigree of baboons. *Human Brain Mapping.* 28:576-583.

Rogers J, Kochunov PV, Zilles K, Shelledy W, Lancaster JL, Thompson P, Duggirala R, Blangero J, Fox PT, Glahn DC. 2010. On the genetic architecture of cortical folding and brain volume in primates. *NeuroImage.* 53:1103-1108.

Rumbaugh DM. 1977. *Language learning by a chimpanzee: The Lana project.* New York: Academic Press.

Sawada K, Sun XZ, Fukunishi K, Kashima M, S. S, Sakata-Haga H, Sukamoto T, Fukui AY. 2010. Ontogenetic pattern of gyrification in fetuses of cynomolgous monkeys. *Neuroscience.* 167:735-740.

Scerrl TS, Morris AP, Buckingham LL, Newbury DF, Miller L, Monaco AP, Bishop DVM, Parachini S. 2011. DCDC2, KIAA0319 and CMIP are associated with reading-related traits. *Biological Psychiatry*. 70:237-245.

Schmitz J, Gunturkun O, Ocklenburg S. 2019. Building an Asymmetrical Brain: The Molecular Perspective. *Front Psychol*. 10:982.

Sha Z, Schijven D, Carrion-Castillo A, Joliot M, Mazoyer B, Fisher SE, Crivello F, Francks C. 2021. The genetic architecture of structural left-right asymmetry of the human brain. *Nat Hum Behav*.

Specht K, Wigglesworth P. 2018. The functional and structural asymmetries of the superior temporal sulcus. *Scand J Psychol*. 59:74-82.

Spocter MA, Sherwood CC, Schapiro SJ, Hopkins WD. 2020. Reproducibility of leftward planum temporale asymmetries in two genetically isolated populations of chimpanzees (*Pan troglodytes*). *Proc Biol Sci*. 287:20201320.

Staes N, Stevens JMG, Helsen P, Hillyer M, Korody M, Eens M. 2014. Oxytocin and vasopressin receptor gene variation as a proximate base for Inter- and intraspecific behavioral differences in bonobos and chimpanzees. *PLoS One*. 9:e113364.

Suwada K. 2020. Cerebral sulcal asymmetry in macaque monkeys. *Symmetry*. 12:1-9.

Warren JM. 1980. Handedness and laterality in humans and other animals. *Physiological Psychology*. 8:351-359.

Weiss A, Wilson VAD, Hopkins WD. 2021. Early social rearing, the V1A arginine vasopressin receptor genotype, and autistic traits in chimpanzees. *Autism Res*. 14:1843-1853.

White T, Su S, Schmidt M, Kao CY, Sapiro G. 2010. The development of gyrification in childhood and adolescence. *Brain Cogn.* 72:36-45.

Wilson VA, Weiss A, Humle T, Morimura N, Usono T, Idani G, Matsuzawa T, Hirata S, Inoue-Murayama M. 2017. Chimpanzee Personality and the Arginine Vasopressin Receptor 1A Genotype. *Behav Genet.* 47:215-226.

Yirmiya N, Rosenberg C, Levi S, Salomon S, Shulman C, Nemanov L, Dina C, Ebstein RP. 2006. Association between the arginine vasopressin 1a receptor (AVPR1a) gene and autism in a family-based study: mediation by socialization skills. *Mol Psychiatry.* 11:488-494.

Zilbovicius M, Meresse I, Chabane N, Brunelle F, Samson Y, Boddaert N. 2006. Autism, the superior temporal sulcus and social perception. *Trends in Neurosciences.* 29:359-366.

Zilles K, Armstrong E, Moser KH, Schleicher A, Stephan H. 1989. Gyrification in the cerebral cortex of primates. *Brain, Behavior and Evolution.* 34:143-150.